

U-Pb zircon xenocrysts dating as a proxy to assess volcanic assimilation and the underlying crust, Cretaceous Jaguarão Formation, RS, Brazil

Vicente Araújo¹ , Juliana Marques¹ , Gabriel Bertolini^{1*} , José Frantz¹ 

Abstract

The Early Cretaceous volcanic Jaguarão Formation formed during the early stages of Gondwana breakup. These felsic rocks characteristically enclose numerous crustal xenoliths. Fieldwork, petrographic studies, and laser ablation multicollector ion coupled plasma mass spectrometer (LA-ICP-MS) U-Pb analyses were carried out to evaluate the xenoliths of the Jaguarão Formation. A base-to-top distribution of xenoliths in the different flows of the volcanic pile indicates that earlier flows incorporated centimeter-sized fragments of local underlying gneiss, granite, and quartz veins, with limited assimilation. In the middle part of the volcanic pile, the size of the xenoliths is smaller and assimilation textures are more frequent. At this same level, reequilibrated orthopyroxene and plagioclase antecrysts were recognized, suggesting fractionation coeval with assimilation in a lower magmatic chamber prior to extrusion. At the top, no visible xenoliths occur. U-Pb ages of the zircon xenocrysts served as a proxy for assessing the crust underlying the volcanic rocks. Most of the ages obtained are similar to the ages of the Eastern Dom Feliciano Belt cropping out nearby, ranging from 680 to 620 Ma, with a subordinate group ranging from 580 to 570 Ma, suggesting a shallow crust contribution. The presence of few Paleoproterozoic and Mesoproterozoic (1.0–1.2 Ma) zircons, however, suggests that the underlying terrain may be more complex.

KEYWORDS: Jaguarão Formation; xenoliths; zircon; U-Pb dating; Dom Feliciano Belt.

INTRODUCTION

The continental crust can be substantially affected by accretion and reworking, and the lower crust might show a more complex age pattern than the exposed upper crust (Tang *et al.* 2014). During ascent, magmas can be contaminated considering the high heat and assimilation of wall-rocks (e.g. Reiners *et al.* 1995, Beard *et al.* 2005, McBirney and Yoder 2015), although the nature of the contaminant might be difficult to recognize. Magmatic rocks with abundant xenoliths offer the opportunity to investigate the nature of the deeper crust and can provide elements for a better understanding of lithospheric evolution.

The genesis of the felsic Early Cretaceous volcanic Jaguarão Formation has been associated with high rates of crustal melting (Vieira Jr. 1985, Vieira and Roisenberg 1987, Comin-Chiaramonti *et al.* 2010) and is interpreted to have been transported through the crust, possibly in the early stages of the

Gondwana breakup (Misuzaki 1998, Comin-Chiaramonti *et al.* 2010). These felsic volcanic rocks characteristically enclose many different types of millimeter to centimeter-sized xenoliths, but the nature and sources of the xenoliths remain unknown.

In order to evaluate the xenoliths of the Jaguarão Formation, fieldwork, petrographic studies, and LA-MC-ICP-MS U-Pb analyses were conducted. U-Pb zircon geochronology of crustal xenoliths has long been used to unravel the evolution of the continental lithosphere (e.g. Rudnick and Williams 1987, Schmitz and Bowring 2001, Davis *et al.* 2003). The ages registered in zircon xenocrysts of the Jaguarão Formation are considered a proxy to assess the underlying crust and the results are compared to the ages of the surface lithostratigraphic units and adjacent tectonic terranes.

TECTONIC SETTING

The Jaguarão Formation represents a felsic volcanic event related to the Wealdenian Reactivation of the South American Platform (Almeida *et al.* 1976), a tectono-magmatic event initiated during the Jurassic and related to the breakup of Gondwana. It is interpreted to be coeval with the Paraná-Etendeka large igneous province, based on an Rb-Sr isochronic age of 139.6 ± 7.4 Ma (Comin-Chiaramonti 2000). The Jaguarão Formation is composed of extrusive rocks, mostly intermediate in composition, dominated by dacites and subordinate rhyodacites with abundant xenoliths (Vieira Jr. 1985, Vieira and Roisenberg 1987, Comin-Chiaramonti *et al.* 2010).

¹Instituto de Geociências, Universidade Federal do Rio Grande do Sul – Porto Alegre (RS), Brazil. E-mails: geohutton@geologia@gmail.com, juliana.marques@ufrgs.br, gabertol@gmail.com, jose.frantz@ufrgs.br

*Corresponding author.

Supplementary material

Supplementary data associated with this article can be found in the online version: [Supplementary Table A1](#)



In the study area, the Dom Feliciano Belt is the most important terrane and is composed mainly of Neoproterozoic granitoids intruded during the Brasiliano-Pan-African Cycle over a NE-SW corridor that extends for ca. 1,200 km, from Punta del Este (Uruguay) to the northeastern portion of the State of Santa Catarina (Brazil) (Fragoso-César 1986, Frantz and Botelho 2000, Philipp and Machado 2002, Basei *et al.* 2011). Archean to Paleoproterozoic terranes occur to the west and to the north, including the Piedras Altas, Nico Perez, and Taquarembó Block (Oyhantçabal *et al.* 2011, Oriolo *et al.* 2016), and the Encantadas and Arroio dos Ratos Complexes (Frantz and Botelho 2000, Saalman *et al.* 2011, Gregory *et al.* 2015), respectively. Minor Mesoproterozoic rocks are only described from the southernmost portion of the study area, from the Cuchilla Dionísio terrane in Uruguay (Bossi and Gaucher 2004, Basei *et al.* 2005, 2011).

The Jaguarão Formation crops out within the Eastern Dom Feliciano Belt (Fig. 1). The rocks are predominantly Ediacaran granitoids, varying from tonalitic to granodioritic

in composition. They were intruded within active shear zones and affected by local mylonitic deformation, and were later followed by late K-feldspar-rich undeformed granites (Frantz and Botelho 2000, Cruz 2019). The granitoids of the Eastern Dom Feliciano Belt include a series of Paleoproterozoic and Tonian inliers (Fragoso-César 1986, Silva *et al.* 1999, Frantz and Botelho 2000, Philipp and Machado 2002). Tonian meta-granitoid inliers (ca. 800–780 Ma) are considered to be related to a tangential regime and possibly to a magmatic arc phase (Frantz and Botelho 2000, Tambara *et al.* 2019). Tonian to Ediacaran metavolcano-sedimentary sequences also occur nearby (Porongos Complex, Höfig *et al.* 2018 and references therein) as well as a Neoproterozoic-Paleozoic sedimentary succession of the Camaquã Basin (Almeida *et al.* 2009).

The local substrate rocks of the Jaguarão Formation are mylonitized biotite monzogranites from the Cerrito Suite (Cruz 2019), considered coeval with the Arroio Pedrado Gneisses (680 ± 2.9 Ma, U-Pb, Vieira *et al.* 2019) located to the north. Granitoids and metagranitoids with a predominance

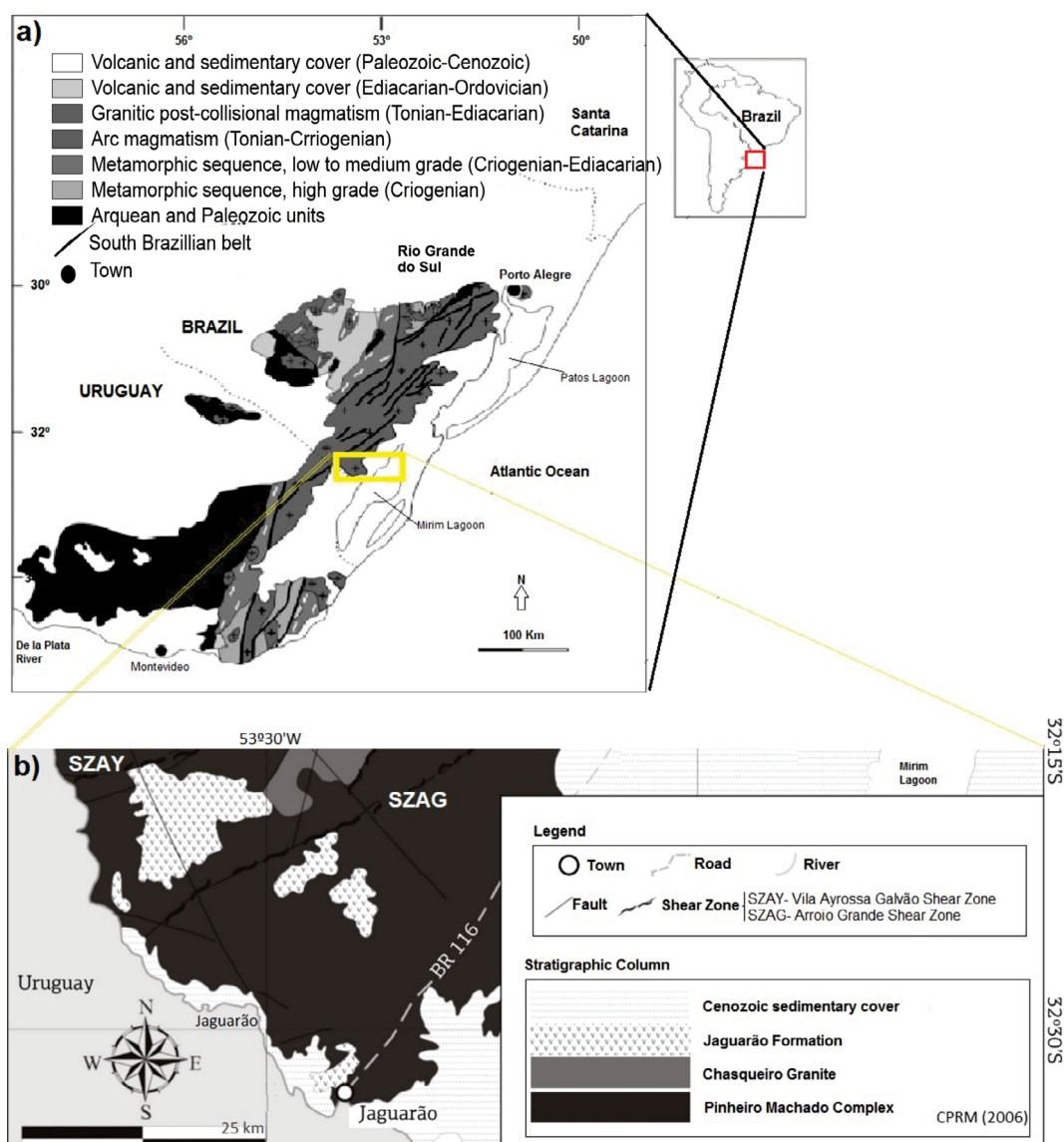


Figure 1. (A) Simplified geological map of the southern portion of the Mantiqueira Province in Southern Brazil and Uruguay showing the location of the studied area (modified from Bitencourt and Nardi 2000); (B) simplified geological map of the studied area (modified from Wildner *et al.* 2008 and Ramos 2014).

of biotite-bearing monzogranite to granodiorites from the Pinheiro Machado Complex occur in the northwestern part, yielding U-Pb ages of 633 ± 4 Ma (Cruz 2019) to 625 ± 4 Ma (Pb/Pb, Philipp and Machado 2002). Late leucogranites and muscovite-biotite granitoids also occur and were included in the Três Figueiras Granite unit, yielding U-Pb ages of 573 ± 5 Ma (Cruz 2019) similar to the ages reported for the northward, for the K-feldspar-rich Chasqueiro Granite (574 ± 3 Ma) (Vieira *et al.* 2016). The Arroio Grande Complex is associated with the shear zones and comprises an association of mafic, ultramafic, and sedimentary metamorphosed rocks interpreted as an ophiolite (Ramos 2014) with a maximum depositional U-Pb derived age of 668 ± 11 Ma (Cruz 2019). A metapelitic to metapsammitic sequence, metamorphosed under amphibolite facies conditions, has also been characterized in the area and named the Arroio Telho Complex, with a maximum depositional age constrained to ca. 636 Ma (U-Pb, Cruz 2019).

The Jaguarão Formation covers a small area, approximately 160 km², with an estimated volume of ca. 3.2 km³ (Comin-Chiaramonti *et al.* 2010). It has an elongated elliptical shape in the NE-SW direction and is 5.5 km long and 1 km wide, constituting the highest relief in the region (Vieira Jr. 1985) (Fig. 1). The volcanic rocks are horizontal and occur directly on basement Proterozoic rocks. The flow successions have a maximum thickness of 40m in the central portion, with a gradual decrease towards their margins (Iglesias *et al.* 2018). A system of columnar joints prevails over horizontal joints, and the absence of amygdaloidal zones is interpreted as a result of either a single effusive process (Vieira Jr. and Roisenberg 1987) or a low volatile content in the magma (Comin-Chiaramonti *et al.* 2010).

Vieira Jr. (1985) proposed that the evolution of the Jaguarão Formation is linked to the NE rift system of the Lagoa Mirim marginal basin. In its Uruguayan portion, this basin records alkali rocks associated with a volcanic sequence ranging from basalts to rhyolites. Most of the basin is covered by Cretaceous sediments aged between 120 and 140 Ma (Umpierre and Halpern 1971, Bossi and Urquhart 1975, Almeida 1983).

Geophysical studies describe positive gravimetric and residual magnetic field anomalies for the Jaguarão region (Rosa *et al.* 2009), with a complex structure and significant compositional heterogeneity. The rifting that led to the opening of the Atlantic Ocean is associated with magmatism, and the E-W Jaguarão Lineament is continuous to the east, associated with positive gravimetric anomalies (Rosa *et al.* 2009), probably indicating that the Jaguarão magmatism is represented by a larger unit not exposed.

The Jaguarão Formation is interpreted as being associated with high rates of crustal melt, based on geochemical evidence (high amounts of incompatible elements and enrichment in light rare-earth elements) and isotopic compositions (high Sr⁸⁷/Sr⁸⁶ initial ratios), followed by fast transport of the magma through the lithosphere (Vieira Jr. 1985, Vieira and Roisenberg 1987, Comin-Chiaramonti *et al.* 2010). The occurrence of orthopyroxene-cordierite as liquidus phases led Comin-Chiaramonti *et al.* (2010) to consider their origin to be associated with friction melting. Depleted mantle extraction age (Nd T_{DM}) model ages range between 2.02 and 2.22 Ga, similar to Nd T_{DM} model ages from basement rocks, which suggests that the volcanic rocks of the Jaguarão Formation

were formed by the melt of the Paleoproterozoic basement or from a magma highly contaminated by host-rocks (Comin-Chiaramonti *et al.* 2010). The isotopic data are distinct from other Early Cretaceous South American platform felsic magmatism, and the source is likely to have been derived from the Dom Feliciano Belt Paleoproterozoic basement (Comin-Chiaramonti and Gomes 2005, Comin-Chiaramonti *et al.* 2010).

MATERIALS AND METHODS

Twenty-two stations were described, including both Jaguarão Formation and basement units (Fig. 2). Thin sections have been described using optical and electronic microscopy (JEOL 6610LV scanning electron microscope with energy dispersive X-ray spectrometry, SEM/EDS) at Laboratório de Geologia Isotópica/Universidade Federal do Rio Grande do Sul (LGI/UFRGS). One sample was selected for U-Pb zircon dating. It was crushed and powdered, and, lastly, sieved to fractions between 74-250 µm. Heavy mineral concentrates were obtained by panning and then subsequently purified using conventional magnetic procedures (Frantz Isodynamic Separator), heavy liquid methods (bromofrom), and handpicking. Zircon grains were selected and set in an epoxy resin mount. The mount surface was polished, exposing the grain cores. A JEOL 6610LV SEM at LGI/UFRGS was used for backscatter imaging. The U-Pb analyses by LA-ICP-MS were carried out using a Finnigan Neptune machine equipped with a 193 nm wavelength Excimer ArF laser ablation system (LA) at LGI/UFRGS. The analyses were performed on single spots of 30 µm, using a repetition rate of 7 Hz, energy of 2 mJ/cm², 40 seconds of ablation time, and 1 second integration times. The Faraday cup configuration of the laser ablation multicollector ion coupled plasma mass spectrometer (LA-ICP-MS) was ²⁰⁶Pb, ²⁰⁸Pb, ²³²Th, and ²³⁸U; and IC's on cup L4 with ²⁰²Hg, ²⁰⁴Pb, and ²⁰⁷Pb. Unknown analyses were bracketed by measurements of the international standard GJ-1 (Jackson *et al.* 2004) at every set of 4 zircon spots and used to estimate the necessary corrections and internal instrumental fractionation. The raw data were corrected offline using an Excel spreadsheet following the procedures of Böhn *et al.* (2009) for background, instrumental mass-bias drift, and common Pb. The ²⁰⁴Pb value was corrected for ²⁰⁴Hg, considering the ²⁰²Hg/²⁰⁴Hg ratio to be 4.355, and the ²⁰⁷Pb/²⁰⁶Pb and ²⁰⁶Pb/²³⁸U ratios were corrected for common Pb using the methods of Stacey and Kramers (1975). Analyses, after blank correction, with a ²⁰⁶Pb/²⁰⁴Pb ratio higher than 3000 were discarded considering possible significant common lead content (see Böhn *et al.* 2009 for further details). The ratios of ²⁰⁶Pb/²³⁸U, ²³²Th/²³⁸U, and ²⁰⁶Pb/²⁰⁷Pb and their absolute errors (1σ) were calculated after blank and ²⁰⁴Pb corrections. The intercept method proposed by Youden (1951) was used assuming linear fractionation of ²⁰⁶Pb/²³⁸U. Ages were calculated using ISOPLOT/Ex (Ludwig 2003). The individual age uncertainties are at 2σ. The calculated ages followed Gehrels' (2014) recommendation, where, for grains older than 1.2 Ga and younger than 1.2 Ga, the ²⁰⁷Pb/²⁰⁶Pb and ²⁰⁶Pb/²³⁸U ages were used, respectively. Kernel Density Estimate plots (using ISOPLOT; Vermeesch 2018) were prepared to visualize the final dataset. Supplementary Table 1 compiles the ages obtained.

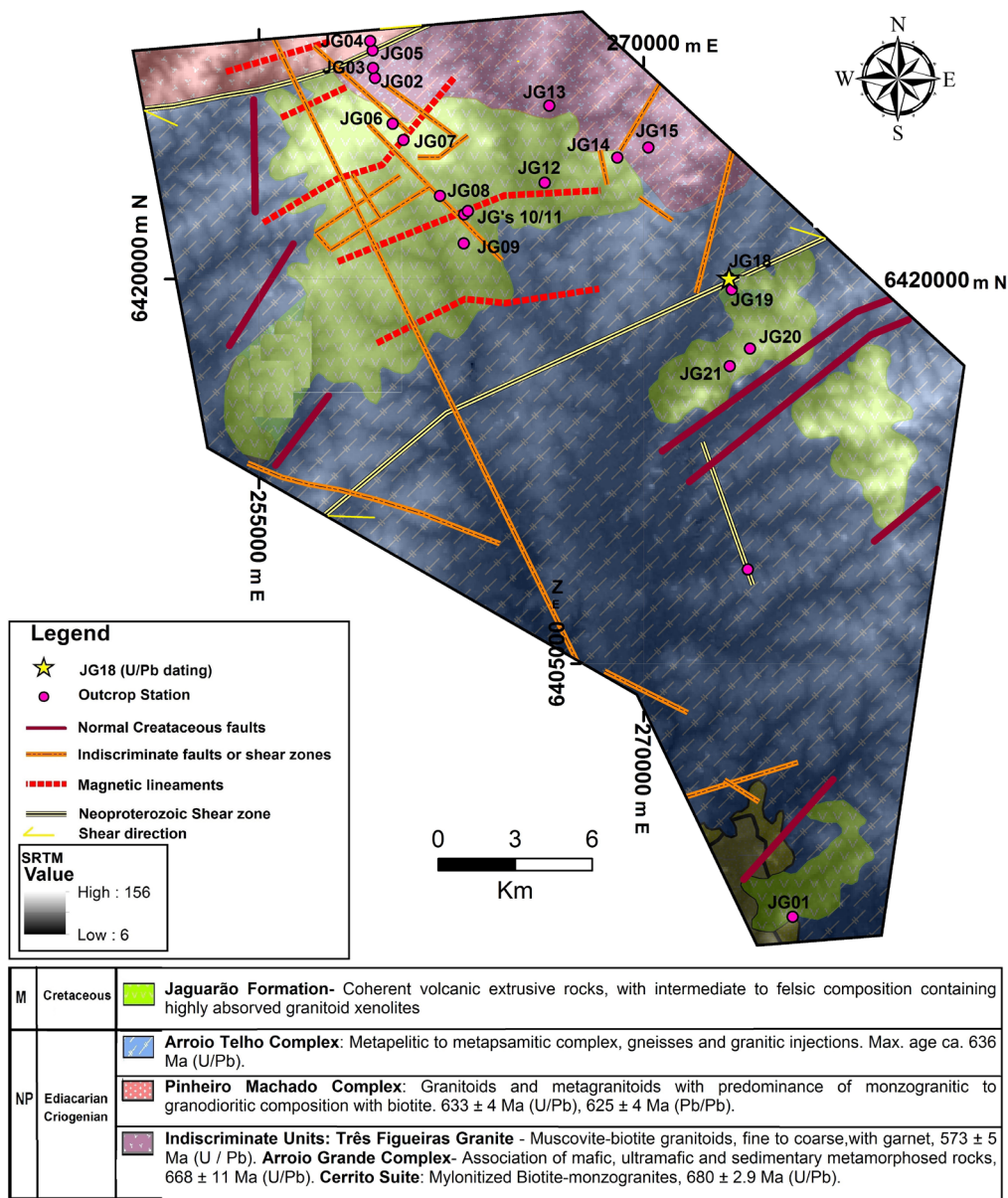


Figure 2. Simplified geological map (modified from Wildner *et al.* 2008, Comin-Chiaromonti *et al.* 2010, Iglesias *et al.* 2018, Cruz 2019) combined with an elevation model showing the field stations.

RESULTS

Basement rocks

The Jaguarão Formation basement is complex and composed of a diversity of rock types. In the studied area, basement outcrops are rare and, generally, highly weathered. Quartz-feldspar gneiss and metagranitoids hosting large fragments of mafic xenoliths, and late intrusive felsic granites are the most common rock types. Figure 3 illustrates the most common basement rocks described in the studied area.

The quartz-feldspar gneiss is medium-grey, characterized by regular millimeter to centimeter-sized mafic banding (up to 2 cm) composed of amphibole and minor biotite, intercalated with thicker (up to 4 cm) felsic bands composed of feldspar (dominantly K-feldspar) and quartz or pure quartz. Mylonitic bands are common. Tight to isoclinal folding is common and highlighted by pure-quartz bands (Fig. 3A). Considering the characteristics, it is probably part of the Arroio Telho Complex.

The metagranitoids predominate and are generally represented by porphyritic biotite metagranitoids with a conspicuous N-NE subvertical foliation marked by the orientation of augen K-feldspar (up to 2 cm in length), biotite, and quartz. This foliation is frequently replaced by a sub-parallel to parallel mylonitic foliation where highly stretched K-feldspar and quartz dominate (Fig. 3B). The intensity of the mylonitization is very high, producing local, meter-scale ultramylonitic zones. Meter to decameter-sized mafic xenoliths are common, and their contacts with the granitic host rocks range from gradational to locally sharp (Figs. 3C and 3D). The mafic xenoliths exhibit a previous well-developed foliation with tight to isoclinal intrafolial folds. Considering the characteristics, the metagranitoids might be part of the Pinheiro Machado Complex.

Late injections of intrusive and undeformed fine-grained granitoids crosscut the metagranitoids and the mafic xenoliths (Figs. 3E and 3F). They are felsic, composed mainly of equigranular K-feldspar and quartz. Pegmatoid veins, similar

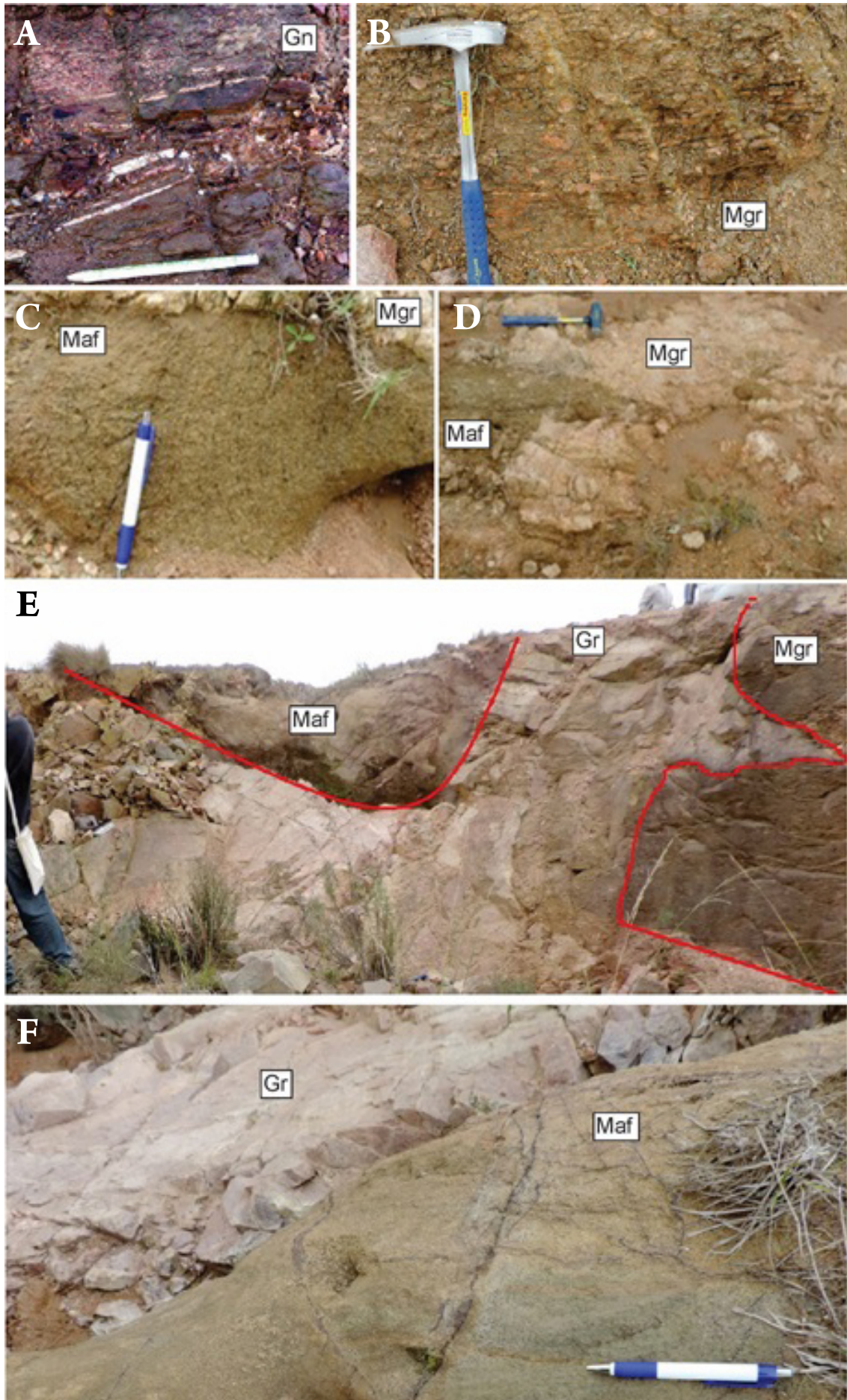


Figure 3. Most common basement rocks of the Jaguarão Formation in the studied area. (A) quartz-feldspar gneiss exhibiting mylonitic microstructure and tight to isoclinal folding (station JG22); (B) porphyritic metagranitoid with subvertical mylonitic microstructure (station JG04); (C and D) metric to decametric mafic xenoliths hosted by metagranitoid (station JG02); (E and F) injections of late intrusive undeformed fine-grained felsic granitoid crosscutting metagranitoid and decametric mafic xenolith (station JG05).

in composition, crosscut all rock types following different directions, but often register subvertical orientations along NE.

The Jaguarão Formation

The Jaguarão Formation crops out as terraces on a flat landform. The rocks are a dark bluish-gray in color with mainly porphyritic textures and aphanitic groundmasses. Near the contact with basement rocks, the rocks are dark gray to black with vitreous groundmasses. The unit displays a dominance of curved vertical planar disjunctions, as well as vertical and horizontal disjunctions (Figs. 4A and 4B). A distinctive feature of these volcanic rocks is the presence of abundant millimeter to centimeter-sized xenoliths of various lithotypes such as gneiss (Fig. 4C), quartz vein fragments (Figs. 4C, 4D and 4E), and fine-grained granite (Fig. 4F). Locally, it

is possible to observe assimilation features such as fragments with irregular margins, gulfs, and embayments. Assimilation features are more frequent where the xenolith sizes are smaller.

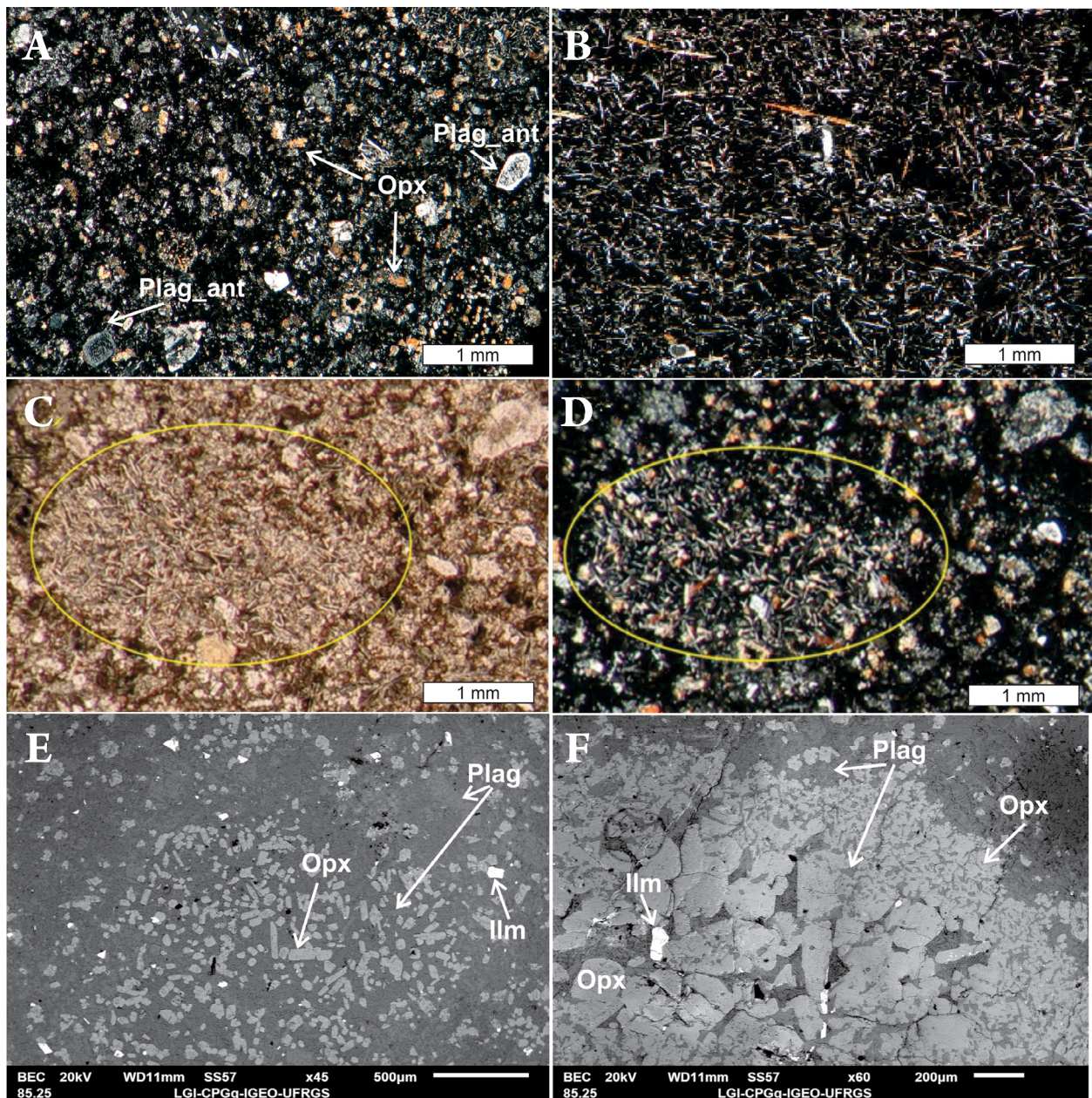
In the field, the Jaguarão Formation shows distinct facies. Rocks of the basal portion of the volcanic pile show a higher degree of crystallinity — with a predominance of fine porphyritic textures and the presence of millimeter-sized vesicles and amygdules. Furthermore, parallel planar vertical structures with pronounced curvature occur frequently (Figs. 4A and 4B). Xenoliths in this portion are centimeter to millimeter-sized and consist mainly of quartz vein fragments, gneisses, and granites (Figs. 4C, 4D and 4E). Locally (one station), an abundance of generally rounded fragments of aphanitic volcanic rocks (average of 30 cm in size) and obsidian fragments immersed in very



Figure 4. General aspects of outcrops and rocks from the Jaguarão Formation. Dark bluish-gray lavas showing (A) curved vertical and (B) vertical planar disjunctions. Abundant xenoliths, millimeter to a centimeter in size, of varied lithotypes such as (C) gneiss, (C, D and E) quartz-rich rock, and (F) fine-grained granite.

fine volcanic and clay-rich material was found. The texture and composition suggest that these fragments are possible autoliths. In the middle part of the volcanic pile, the abundance of xenoliths increases in the rocks, frequently showing assimilation features such as irregular margins and embayments and bounded by aphanitic groundmass. The dominant xenoliths are undeformed leucogranites, varying from angular to rounded (Fig. 4F). In the upper part of the volcanic pile, it is common to find fine-grained dark gray to black rocks with very fine-grained or even aphanitic textures, and very few millimeter-sized vesicles and amygdules. It is worth noting the absence of visible xenoliths or, at most, the presence of very few tiny xenoliths at this level.

Microscopically, the volcanic rocks of the Jaguarão Formation have dominantly porphyritic textures (Fig. 5A) with local very fine-grained textures (Fig. 5B), with orthopyroxene and ripiform plagioclase phenocrysts varying from 1 mm to less than 0.1 mm-long immersed in either dark grey vitreous or dark-grey aphanitic groundmasses. Larger and non-ripiform plagioclase crystals (up to 0.5 mm) also occur and are zoned with more calcic cores showing local dissolution followed by a more homogeneous and sodic rim (Fig. 5A). These characteristics are suggestive of prior crystallization under distinct magmatic composition/conditions, implying that these types of plagioclases could actually be antecrysts (cf. Davidson *et al.* 2007, Jerram and Martin



Plag_X: plagioclase xenocryst; Plag: plagioclase; Opx: orthopyroxene; Ilm: ilmenite.

Figure 5. General petrographic features of the Jaguarão Formation volcanic rocks. Photomicrographs of (A) typical porphyritic texture with plagioclase antecrysts, (B) fine-grained porphyritic texture and fine-grained porphyritic autolith, (C and D) with an elliptical shape and irregular boundaries, all composed of euhedral prismatic crystals of orthopyroxene and plagioclase immersed in a vitreous groundmass. Backscattering images of (E) orthopyroxene, plagioclase and minor ilmenite glomerophyre and (F) orthopyroxene-rich glomerophyre with spongy orthopyroxene in the outer margins.

2008). Small autoliths (3 to 5 mm) with a very fine-grained porphyritic texture also occur, composed of aphanitic to vitreous groundmass with 0.1 to 0.3 mm-long phenocrysts of orthopyroxene and ripiform plagioclase. The autoliths are enclosed by porphyritic rock and show irregular boundaries (Figs. 5C and 5D).

The orthopyroxene phenocrysts are tabular, euhedral, and with dimensions between 0.3 mm and 0.1 mm (Fig. 5A). Furthermore, orthopyroxene also occurs in the groundmass as idiomorphic crystals, prismatic, and with mean dimensions around 0.03 mm. SEM/EDS analyses suggest an intermediate composition with an Mg ratio (Mg/Mg+Fe) between 0.50 to 0.60 and very low Ca.

The plagioclase phenocrysts are prismatic and euhedral, with dimensions between 0.5 mm and 0.25 mm (Fig. 5A). SEM/EDS analyses suggest an intermediate composition (ca. 50% An). Plagioclase also occurs as elongated microcrystals in the groundmass, showing acicular shapes, with average dimensions of 0.03 mm (Fig. 5B). Plagioclase phenocrysts occur in equilibrium with orthopyroxene phenocrysts.

The groundmass is dark-gray, generally aphanitic. The aphanitic groundmass has a fine hypocrySTALLINE texture, represented partly by crystals and partly by glass (Fig. 5B).

The orientation of plagioclase and orthopyroxene phenocrysts and microphenocrysts is usually random but local preferential orientation does occur, with the development of a trachytic texture.

The autoliths are generally elliptical in shape and elongated, having irregular contacts with the surrounding material (Figs. 5C and 5D). Autoliths have a fine porphyritic texture composed of very small prismatic orthopyroxene and plagioclase phenocrysts in a vitreous groundmass.

Glomeroporphyritic texture composed mainly of orthopyroxene, plagioclase, and minor ilmenite occurs in some volcanic layers (Fig. 5E). Orthopyroxene-rich glomerophyre also occurs (Fig. 5F). At the margins the large orthopyroxene crystals (up to 0.5 mm) show absorption, exhibiting a spongy texture. The spongy-textured orthopyroxene is associated with more significant amounts of anhedral plagioclase. No cordierite was identified in our samples, although previous work (Comin-Chiaramonti *et al.* 2010) has reported its presence.

Xenoliths

Xenoliths are widely found in the Jaguarão Formation, varying from millimeter to centimeter-sized fragments of distinct lithotypes such as milky quartz, quartz mylonite, granitoids, metagranites, and gneisses and, less commonly, schists. The occurrence of larger xenoliths is more frequent in the vicinity of the contacts with the substrate rocks (Fig. 4D), whereas xenocrysts and xenoliths with assimilation textures are more common in the middle part of the volcanic succession.

Xenoliths with angular or rounded shapes composed of quartz aggregates are the most common (Figs. 6A, 6B, 6C and 6D). The quartz aggregates show strong undulatory extinction (Figs. 6B, 6C and 6D). These xenoliths have well-defined boundaries and are surrounded by reaction halos marked by an

increase in proportion and size of orthopyroxene phenocrysts associated with plagioclase and vitreous groundmass (Figs. 6E and 6F). Irregular fractures that are interconnected and filled with volcanic material occur, indicating partial assimilation (Fig. 6E).

Granitoid xenoliths also occur. They are mostly represented by leucogranites with fine-grained equigranular textures, with less than 1% of mafic minerals. The leucogranite xenoliths are generally spherical to amoeboid in shape and show pristine boundaries with no evidence of assimilation. Metagranites and gneiss xenoliths are also frequently found. These xenoliths show well-developed foliation and bands composed of aligned K-feldspar and biotite aggregates, in discontinuous or dispersed areas. These xenoliths have irregular, diffuse, and assimilated boundaries.

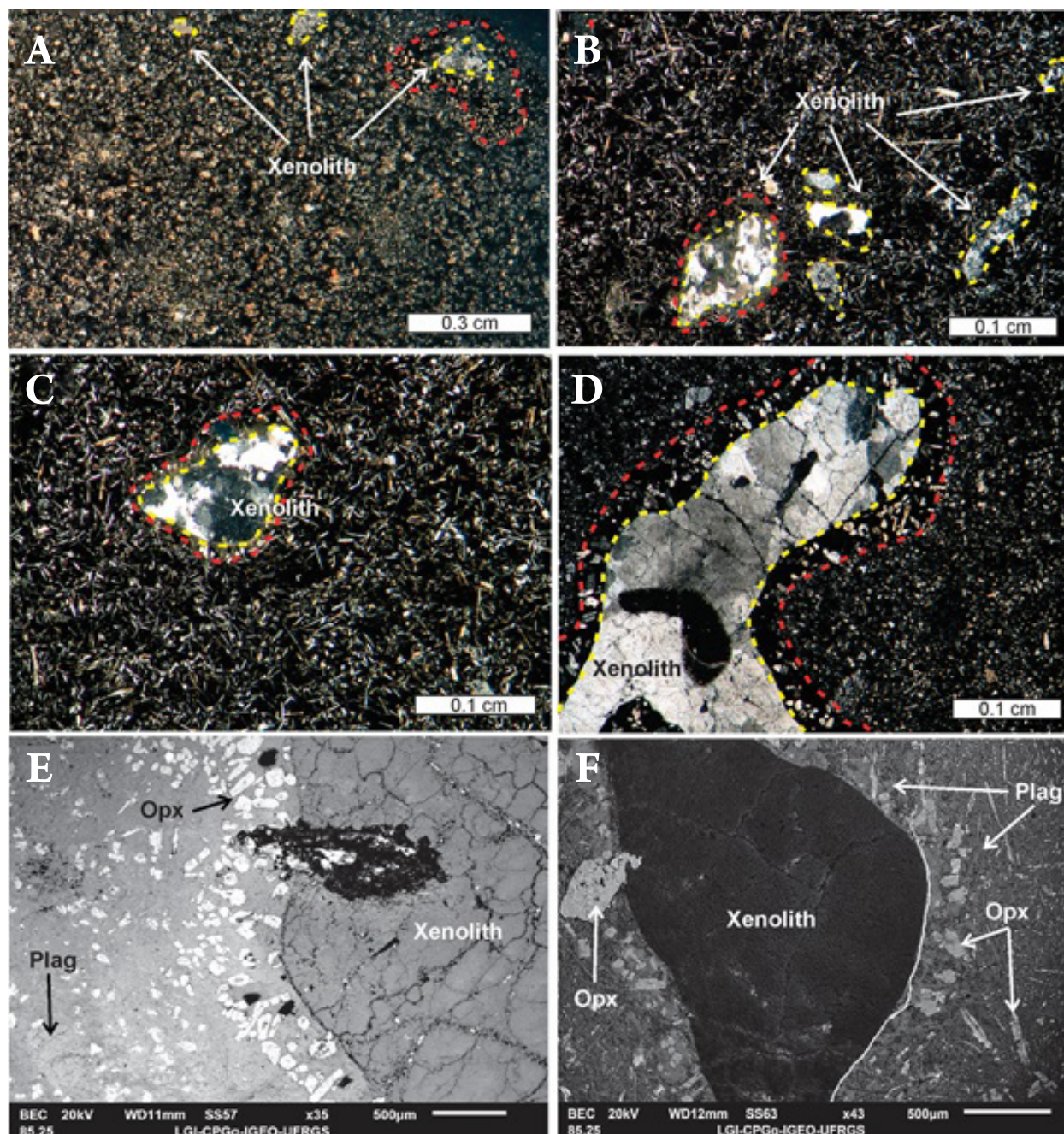
In the middle of the volcanic pile, fewer macroscopic xenoliths occur in the rocks. On the other hand, higher proportions of zircon xenocrysts, exhibiting distinct morphologies, are recognized. Figure 7 compiles the vertical variation of the types of xenoliths and petrographic features of the Jaguarão Formation rocks.

Zircon xenocrysts morphology and U-Pb dating

The petrographic characterization of the rocks of the Jaguarão Formation aided in the selection of a representative sample to be used for U-Pb zircon dating. Sample JG18B was selected considering the absence of visible xenoliths but with a larger number of zircon xenocrysts. The absence of visible xenoliths and the exclusive presence of microxenoliths and xenocrysts suggest that enough time had elapsed, and the necessary thermal conditions had occurred, to produce more complete assimilation of rock fragments. We considered that this could increase the possibility that these zircon xenocrysts represent a deeper crust contribution.

The selected sample yielded different populations of zircons. Figure 8 illustrates the most common types of zircon xenocrysts recovered. Zircons crystals are euhedral to rounded in shape, ranging from 40 to 200 μm in size with an aspect ratio from 4:1 to 1:1. The euhedral crystals (Figs. 8A, 8B, 8C and 8D) are translucent, vary from 25 to 80 μm in length and display length/width ratios of 4:1, with well-formed prisms and short bi-pyramidal terminations partially rounded (Figs. 8A and 8D). Twinned zircons also occur (Fig. 8C). The rounded populations display shorter aspect ratios (2:1 to 1:1), fractured grains, and corroded edges (Figs. 8E, 8F, 8G and 8H). Rounded grains also show dissolution features (Figs. 8F and 8G), similar to those described for the xenoliths. The crystals are generally colorless, with some grains showing a matte appearance. Furthermore, the grains display features such as micro-fractures and porosity (Figs. 8E, 8F and 8G), inclusions, and metamictic effects. Oscillatory zoning occurs (Figs. 8C and 8D) mostly in euhedral grains, while the rounded grains tend to present patchy to sectorial zoning (Fig. 8G).

Thirty-one U-Pb ages were obtained through LA-MC-ICP-MS analysis. The results reveal ages between 2.02 to 0.53 Ga, with a predominance of crystals with ages ranging



Plag: plagioclase; Opx: orthopyroxene.

Figure 6. General petrographic features of the xenoliths of the Jaguarão Formation. (A, B, C and D) Photomicrographs of the typical quartz-rich xenoliths with lobed boundaries (highlighted by yellow dashed lines), partial absorption, and reaction halos (outer limits highlighted by red dash lines). (E and F) Backscattering images of the xenoliths showing the reaction halos composed of more abundant and larger orthopyroxene phenocrysts associated with plagioclase immersed in a vitreous groundmass. Fractures filled with volcanic material (F) illustrate the assimilation process.

from 0.84 to 0.53 Ga. The analyzed zircons have low Th/U values ranging from 0.03 to 1.21, where the average varies from 0.1 to 0.5. The ages have been calculated using the IsoplotR package (Vermeesch 2018), an R implementation based on the classic Isoplot of Ludwig (2003). Figure 9 shows the distribution of the analyzed zircons with the Concordia diagram and a pie chart diagram showing the percentage of distinct age populations. Analyses with more than 10% of discordance between $^{207}\text{Pb}/^{206}\text{Pb}$ and $^{206}\text{Pb}/^{238}\text{U}$ were not included in the diagrams (7 grains) (Suppl. Tab. 1).

The most abundant population of ages was between 680 to 620 Ma representing almost 50% of the total analyzed zircons. Zircons with ages between 800 and 720 Ma and zircons with

ages between 580 and 570 Ma represent circa 14% of the total analyzed zircons for each group. Paleoproterozoic zircons represented only 6% of the total, while Mesoproterozoic ages were 8% of the total analyzed zircons. Zircon population with ages younger than 530 Ma was 11% of the total analyzed zircons.

The kernel density plot (Fig. 10A) and the histogram plot (Fig. 10B) show age distributions obtained for the Jaguarão Formation zircon xenocrysts and correlate them with the crystallization ages of the local basement units (Vieira *et al.* 2016, Cruz 2019) and major granitoid intrusion events of the Eastern Dom Feliciano Belt. Figure 11 displays the distribution of the Th/U ratio of the zircon xenocrysts of the Jaguarão Formation. Figure 11 also shows the interval of the Th/U ratio of zircons

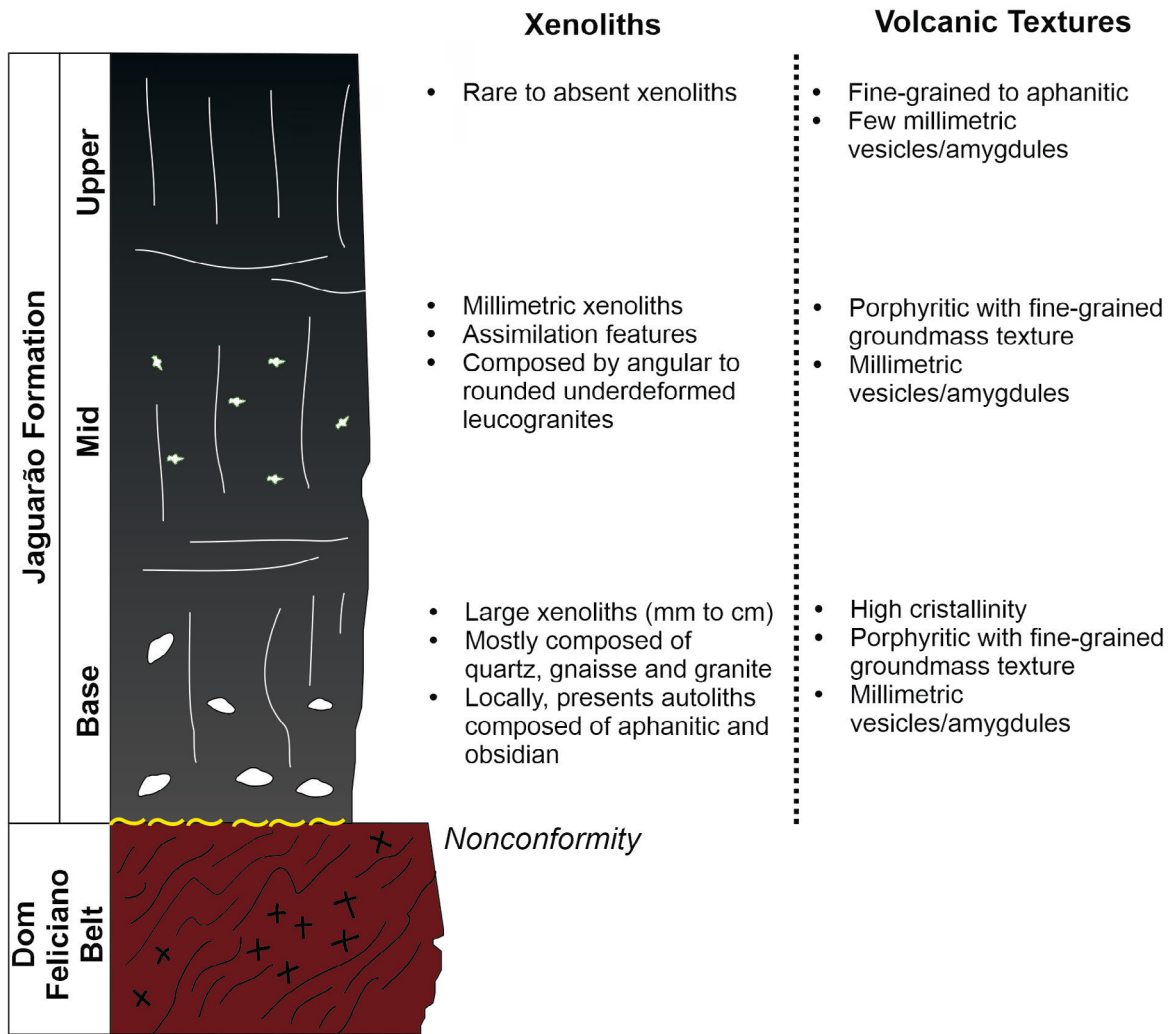


Figure 7. Schematic xenoliths distribution and volcanic textures along the volcanic succession flows of the Jaguarão Formation. The figure is out of scale.

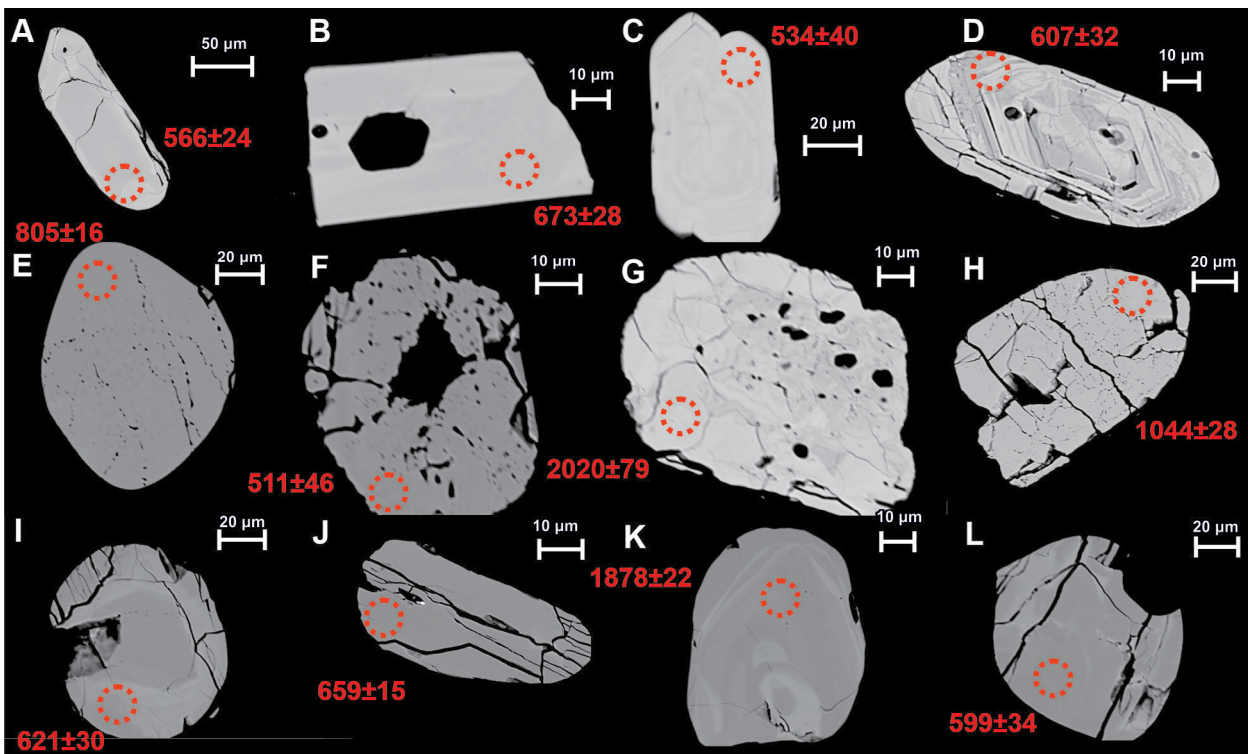


Figure 8. Backscattering images of the different types of zircon xenocrystals and their U/Pb ages (in Ma). (A-D) euhedral elongated grains; (E-L) dissolved zircons.

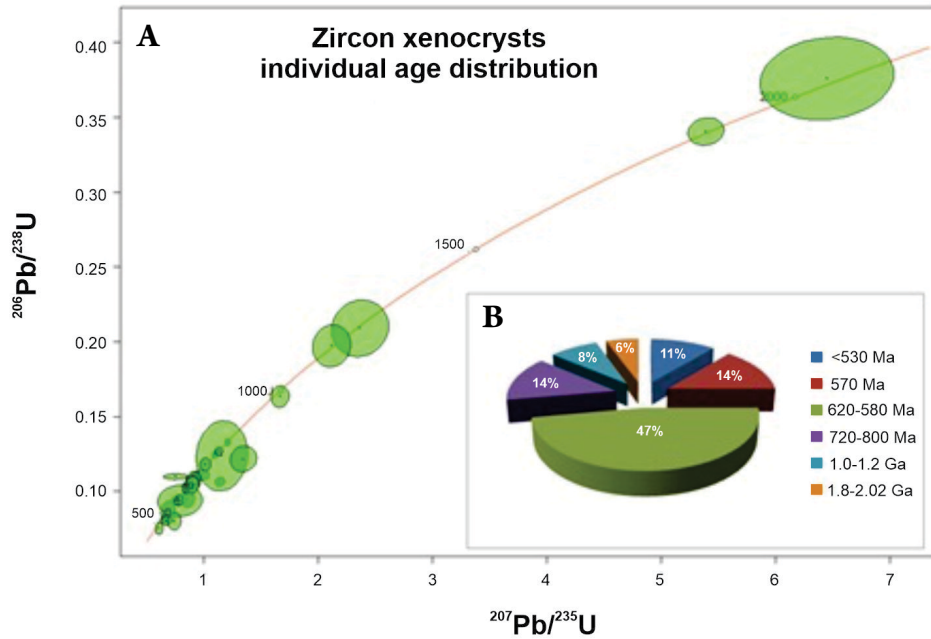


Figure 9. (A) Concordia diagram and a (B) pie-chart diagram showing the distribution of zircon xenocrysts.

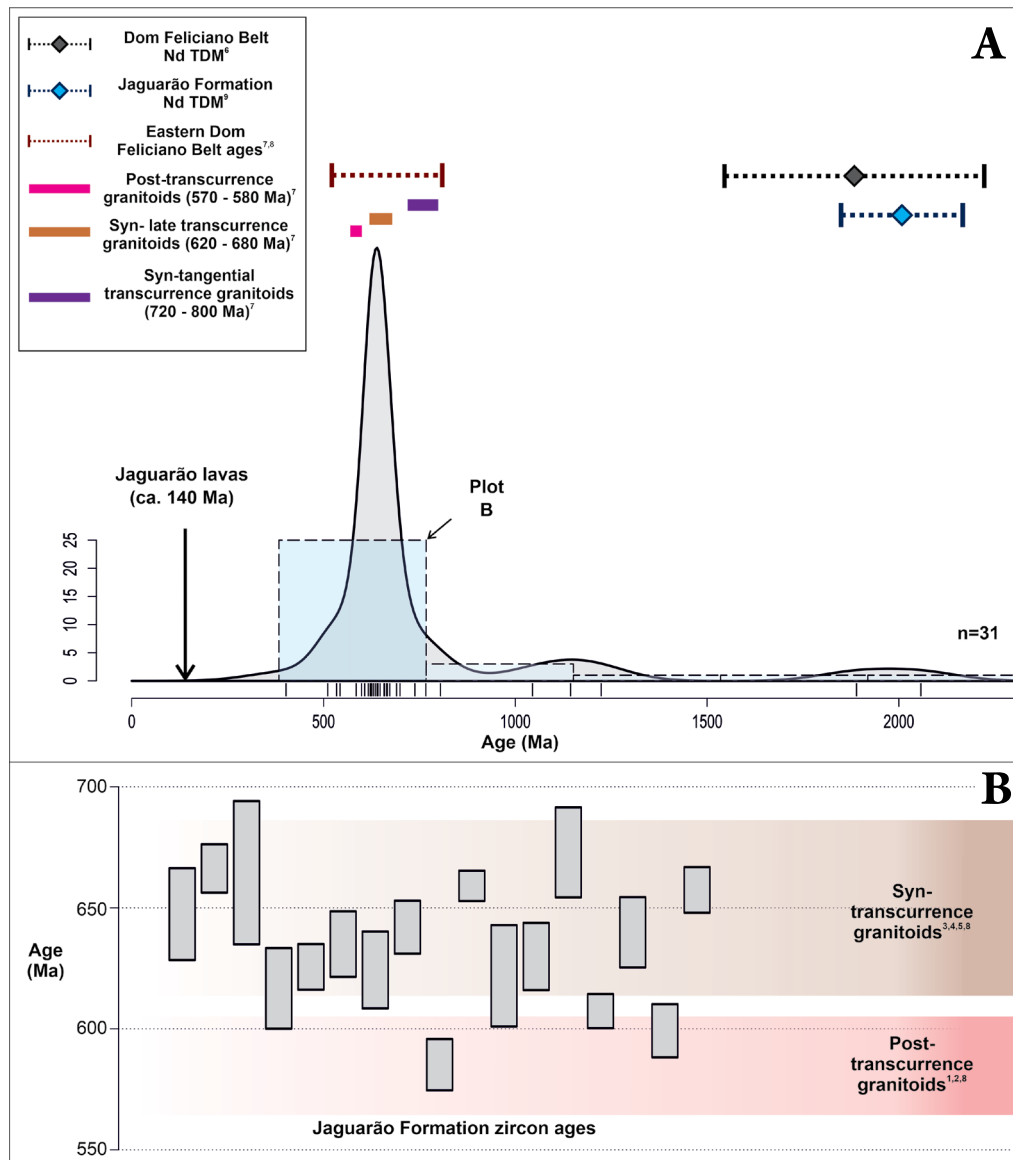
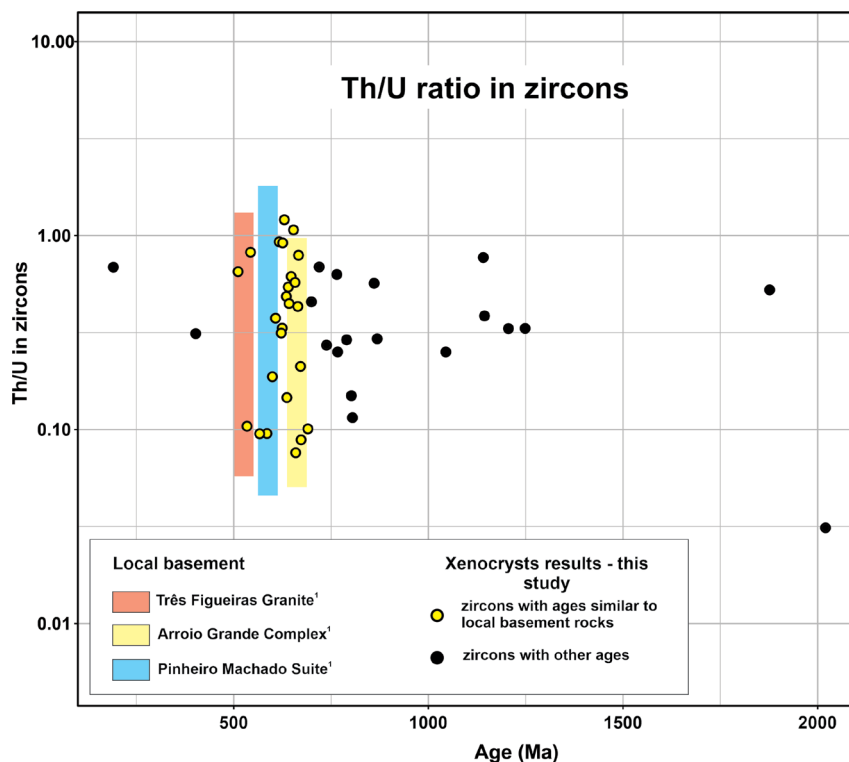


Figure 10. Kernel density estimator (KDE) and (A) histogram plot and (B) weighted mean for sample JG18-BIL. The plots incorporate the Dom Feliciano Belt ages, and data from post- to syn-transpressional granitoids, where: (1) Chasqueiro Granite (Vieira *et al.* 2016); (2) Três Figueiras Granite (Cruz 2019); (3) Arroio Grande Complex (Cruz 2019); (4) Cerrito Suite (Cruz 2019); (5) Arroio Telho Complex (Cruz 2019); (6); Dom Feliciano Belt Nd T_{DM} ages (7 and 8) Dom Feliciano Belt U-Pb ages (Frantz and Botelho 2000, Frantz *et al.* 2003); (9) Jaguarão Nd T_{DM} ages (Comin-Chiaramonti *et al.* 2010).



¹Cruz (2019).

Figure 11. Zircon Th/U comparison of xenocrysts from the Jaguarão Formation and local host-rocks.

from local basement sources (Vieira *et al.* 2016, Cruz 2019). The good correlation of the ages and Th/U ratio distribution between zircon xenocrysts and zircons from local basement rocks corroborates the contribution of local sources. Nd T_{DM} ages of the Jaguarão lavas (Comin-Chiaramonti *et al.* 2010) and the Eastern Dom Feliciano Belt (Frantz and Botelho 2000, Frantz *et al.* 2003, Vieira *et al.* 2016, Cruz 2019) are shown in the blue- and black-dashed bars, respectively. The main zircon peak age matches the majority of the Neoproterozoic metagranitoids and granitoids of the Eastern Dom Feliciano Belt (Frantz and Botelho 2000, Frantz *et al.* 2003, Vieira *et al.* 2016, Cruz 2019), as illustrated by the brown-dashed bar in the kernel density plot (Fig. 10A). Tonian ages and a smaller contribution of Mesoproterozoic and Paleoproterozoic ages were also recognized.

DISCUSSION

Assimilation processes within the Jaguarão Formation

The Jaguarão Formation was previously interpreted as being associated with high rates of crustal melting in the early stages of the Gondwana breakup (Comin-Chiaramonti *et al.* 2010). The presence of cordierite, considered magmatic in origin and equilibrium with orthopyroxene, together with Nd-Sr isotopic signatures similar to those found in the Dom Feliciano Belt granitoids, led Comin-Chiaramonti *et al.* (2010) to this interpretation. Although this evaluation might be correct, it is important to consider that the relatively evolved chemical composition of the dacitic rocks makes it difficult to constrain

melt sources. Mantle-derived magmas, during ascent, can be highly contaminated considering the heat involved and the possible assimilation of wall-rocks (e.g. Reiners *et al.* 1995, Beard *et al.* 2005, McBirney and Yoder 2015). Fractional crystallization and open system processes hamper the reconstruction of the original chemical signature of the parental melt (e.g. Maier *et al.* 2000, Charlier *et al.* 2005, Davidson *et al.* 2007).

The Jaguarão Formation comprises a volcanic succession with varying amounts and types of xenoliths (Vieira Jr. 1985, Vieira and Roisenberg 1987, Comin-Chiaramonti *et al.* 2010). Our field observations allowed the identification of a pattern of distribution of the different types and sizes of xenoliths. A base-to-top distribution of the xenoliths suggests that the volcanics near the base, and those in direct contact with substrate rocks, have possibly incorporated fragments from local underlying rocks considering they show larger xenoliths, many with sharp edges, including quartz veins, granitoids, and gneisses that are common rocks in local basement outcrops. On the other hand, toward the top of the volcanic pile, small xenoliths, predominantly of leucogranites, are more frequent and some volcanic rocks have only microxenoliths and xenocrysts. Evidence of assimilation is common (e.g. Fig. 6), and rocks with a higher number of assimilation features also include a small number of glomeroporphyritic orthopyroxene reequilibrated at their margins, as well as plagioclase antecrysts.

Assimilation of country rocks is a widespread process in different types of magmatic systems (e.g. Sparks 1986, Reiners *et al.* 1995, Maier *et al.* 2000, Kuritani *et al.* 2005, Solano *et al.* 2012, Yao *et al.* 2021), where the fragments of rock can dissolve, disintegrate, or even melt and blend with

the original melt (Streck 2008). During this process, it is common to disperse xenocrysts and add melt to the formerly uncontaminated magma depending on the composition and temperature, which produces complex features and petrological evolution (Sparks 1986, Reiners *et al.* 1995, Jerram and Davidson 2007, Streck 2008, Azzone *et al.* 2020, Yao *et al.* 2021). Ultimately, the rate of assimilation is a factor of physical and chemical processes, a complex subject. According to Clarke (2007), the reaction rate is increased by xenolith physical breakage, resulting in higher ratios of crystal surface to magma volume. Chemical processes are dependent on magma temperature, the ratio of magma/xenoliths (concentration of reactants), mineral activation energies, chemical diffusivity, and fluid concentration. Although our study is not in-depth from the petrological point of view, the presence of larger and more variable xenoliths with low degrees of assimilation, suggestive of local fragments incorporation at the base of the volcanic pile, and small fragments that are highly assimilated towards the top, might indicate more than one stage of contamination. Zircon xenocrysts showing dissolution features occur in some volcanic rocks (e.g. Figs. 8F and 8G), which suggests a higher degree of assimilation compared to rocks with larger preserved xenoliths at the base. Zircon dissolution is important because the mineral usually shows low solubility (e.g., Watson 1996, Harley and Kelly 2007). The survival of zircon xenocrysts might imply that these crystals resided in a highly crystalline mush (e.g., Cooper and Kent 2014). The presence of glomeroporphyritic texture with orthopyroxene reequilibrated at its margins together with the plagioclase antecrysts in the same volcanic rocks that host larger amounts of zircon xenocrysts corroborates a magmatic chamber where fractionation and assimilation occurred before the volcanic eruption. Antecryst populations might indicate crystallization stages in a magma chamber at lower levels (e.g. Azzone *et al.* 2020). Our data suggest that the magma has experienced both assimilation and crystallization in a magma chamber before extrusion and, possibly, has suffered more than one stage of contamination incorporating fragments of local basement rocks in the earlier eruptions. However, due to the complexity of the subject, this last suggestion should be considered with caution.

Zircon U-Pb ages as a proxy for xenolith contribution

The U-Pb dating of zircon xenocrysts might work as a proxy to assess the crust (Harley and Kelly 2007) underlying the volcanic rocks. The U-Pb ages obtained for xenocrysts of the Jaguarão Formation were analyzed to correlate the results with the ages of local substrate rocks cropping out nearby, belonging to the Dom Feliciano Belt. The aim was to constrain possible crustal sources in terms of age. Our results (Figs. 10A and 10B) show that the age distribution of the zircon xenocrysts correlates well with the crystallization ages of the local underlying units (Vieira *et al.* 2016, Cruz 2019) and major granitoid intrusion events of the Eastern Dom Feliciano Belt. The main zircon peak age matches the majority of the Neoproterozoic metagranitoids and granitoids of the Eastern Dom Feliciano Belt. Tonian ages and a minor

contribution of Mesoproterozoic and Paleoproterozoic ages were also identified.

Our U-Pb age dating of zircon xenocrysts reveals a predominance of ages ranging from 680 to 620 Ma, representing circa 50% of the total analyzed crystals with a subordinate group ranging from 580 to 570 Ma (Figs. 9 and 10A). The interval of 680 to 620 Ma is linked to the syn-transcurrence event that is documented for the Eastern Dom Feliciano Belt (Frantz and Botelho 2000, Frantz *et al.* 2003, Vieira *et al.* 2019). The interval of 580 to 570 Ma, locally characterized by the Três Figueiras and Chasqueiro Granite (Vieira *et al.* 2016, Cruz 2019), represents the quiescence of the transcurrent movement and the intrusion of post-tectonic granitoids (Frantz and Botelho 2000, Frantz *et al.* 2003, Vieira *et al.* 2019). The predominance of xenocrysts from these two periods of time and the extensive occurrence of rocks from that age cropping out in the area imply that most xenoliths and preserved xenocrysts in the Jaguarão volcanic rocks are derived from shallow crustal levels, with ages similar to that of the rocks that are currently found in the area. The small *n* of zircons in the samples from the Jaguarão Formation may preclude the definition of additional age peak contributions. Nevertheless, the zircon dating successfully displays the multiple age contributions.

The Paleoproterozoic T_{DM} ages of the Jaguarão rocks were previously interpreted as a consequence of direct melting of the Paleoproterozoic basement or extensive contamination in the magma (Comin-Chiaramonti *et al.* 2010). However, it is complicated to assume any of those processes based solely on T_{DM} ages considering crustal contamination might imprint substantial modifications in depleted-mantle Nd model ages (Azzone *et al.* 2020). Our data revealed just a few Paleoproterozoic xenocrysts despite the high number of xenoliths hosted by the volcanic rocks. The majority of zircon xenocrysts are Neoproterozoic which correlates well with Eastern Dom Feliciano rocks cropping out in adjacent areas. The T_{DM} ages of the Neoproterozoic Eastern Dom Feliciano granitoids are also Paleoproterozoic (Frantz and Botelho 2000, Frantz *et al.* 2003, Vieira *et al.* 2016, Cruz 2019). Considering this scenario, extensive contamination can be considered more plausible, as it could explain both the high amount of Neoproterozoic zircon xenocrysts and the Paleoproterozoic T_{DM} ages of the Jaguarão Formation rocks. On the other hand, the Paleoproterozoic basement is well documented in the Sul-Riograndense Shield, as basement inliers represented by ages ranging from 2000 to 2250 Ma (Saalman *et al.* 2011), and in Uruguay, in the Nico Perez Terrane, where Archean and Rhyacian ages are described (Oriolo *et al.* 2019 and references therein). Melting of Paleoproterozoic or even older basement rocks cannot be disregarded. Figure 12 illustrates the envisaged evolution of the Jaguarão Formation.

The presence of zircon xenocrysts with ages between 1.0–1.2 Ga is an interesting finding considering the scarce geological record of this age interval in the southeastern portion of South America (Basei *et al.* 2011) and suggests the possible presence of

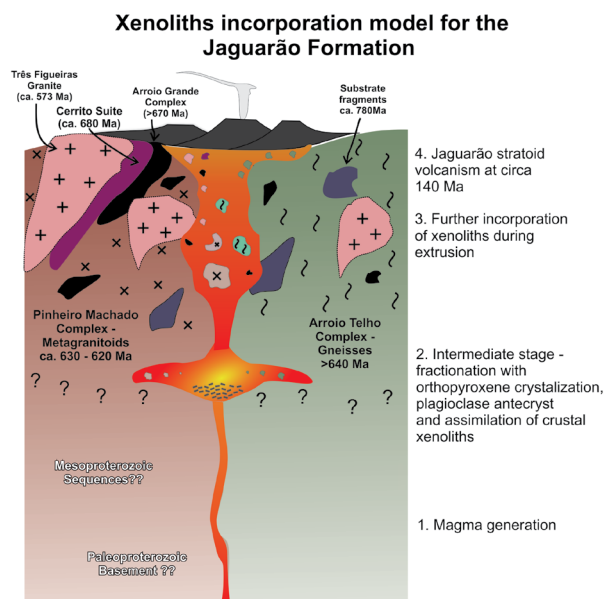


Figure 12. Jaguarão Formation magmatic evolution based on our data and data from previous work (Vieira Jr. 1985, Comin-Chiaramonti *et al.* 2010). Approximate ages from local basement rocks are from Silva *et al.* (1999), Philipp and Machado (2002), Vieira *et al.* (2016), Iglesias *et al.* (2018), Cruz (2019).

Mesoproterozoic rocks in the crust below the Jaguarão Formation. Mesoproterozoic ages in the Eastern Dom Feliciano Belt are not common and no unit has been recognized in adjacent areas so far, although rare Mesoproterozoic ages have already been reported from detrital zircons such as in the Porongos Complex (Höfig *et al.* 2018) located in the Dom Feliciano Belt's northwestern region. On the other hand, Mesoproterozoic ages are recognized in Uruguay at the Punta del Este (Basei *et al.* 2011) and Nico Perez (Oriolo *et al.* 2019) terranes.

CONCLUSIONS

The Jaguarão Formation felsic volcanic rocks have enclosed lots of different types of millimeter to

centimeter-sized xenoliths. Rocks with largely assimilated xenoliths also include small amounts of glomeroporphyritic orthopyroxene reequilibrated at their margins, plagioclase antecrysts, and large amounts of zircon xenocrysts. The fractionation possibly has occurred coeval with the assimilation of crustal fragments in a lower-level magmatic chamber, and the magma also incorporated further fragments either on its way to the surface or during extrusion eroding underlying rocks as evidenced by the presence of larger xenoliths less affected by assimilation processes and similar to basement rocks cropping out nearby. Therefore, our data suggest that more than one stage of crustal contamination occurred and the magma experienced some residence time at an intermediate level before the eruption. The zircon xenocrysts U-Pb ages serve as a proxy for assessing the crust underlying the volcanic pile. Our results reveal that most zircon inclusions in the magma originated in shallow rocks from the Eastern Dom Feliciano Belt. The majority of the zircon xenocrysts have the same ages as that of the local substrate rocks cropping out in the area. However, we envisage a more complex underlying terrain including both Mesoproterozoic and Paleoproterozoic rocks, considering that xenocrysts of these ages were also recovered even though there are no rocks of this age found in the local substrate, although they may occur in neighboring terranes. The presence of 1.0 to 1.2 Ma xenocrysts is an important finding due to the scarce record of this age interval in Southeastern South America.

ACKNOWLEDGMENTS

This work is part of the Master Dissertation of Vicente Medeiros Leivas Araújo. The authors gratefully acknowledge the support received from the Universidade Federal do Rio Grande do Sul. Juliana C. Marques thanks the CNPq for research fellow support (309519/2018-7 and 316460/2021-4), and Gabriel Bertolini thanks the CAPES PrINT for post-doctoral fellowship support (88887.583254/2020-00).

ARTICLE INFORMATION

Manuscript ID: 20210063. Received on: 30 NOV 2020. Approved on: 12 APR 2022.

How to cite this article: Araújo V, Marques J, Bertolini G, Frantz J. U-Pb zircon xenocrysts dating as a proxy to assess volcanic assimilation and the underlying crust, Cretaceous Jaguarão Formation, RS-Brazil. *Brazilian Journal of Geology*, 52(3):e20210063, 2022. <https://doi.org/10.1590/2317-488920220210063>

V.A., J.M., and G.B. wrote the first draft of the manuscript and prepared the figures. J.F. gave advisership regarding basement geology, and improved the manuscript through suggestions and revision; J.M. and G.B. revised and improved the final version of the manuscript.

REFERENCES

- Almeida F.M. 1983. Relações tectônicas das rochas alcalinas mesozóicas da região meridional da Plataforma Sul-Americana. *Revista Brasileira de Geociências*, **13**(3):139-158.
- Almeida F.F., Hasui Y., Brito Neves B.B. 1976. The upper Precambrian of South America. *Boletim IG*, **7**:45-80. <https://doi.org/10.11606/issn.2316-8978.v7i0p45-80>
- Almeida R.P., Janikian L., Fragoso-Cesar A.R.S., Marconato A. 2009. Evolution of a rift basin dominated by subaerial deposits: The Guaritas Rift, Early Cambrian, Southern Brazil. *Sedimentary Geology*, **217**(1-4):30-51. <https://doi.org/10.1016/j.sedgeo.2009.01.010>
- Azzone R.G., Chmyz L., Guarino V., Alves A., de Barros Gomes C., Ruberti E. 2020. Isotopic clues tracking the open-system evolution of the Ponte Nova mafic-ultramafic alkaline massif, SE Brazil: The contribution of Pb isotopes. *Geochemistry*, **80**(4):125648. <https://doi.org/10.1016/j.jchemer.2020.125648>
- Basei M.A.S., Frimmel H.E., Nutman A.P., Preciozzi F., Jacob J. 2005. A connection between the Neoproterozoic Dom Feliciano (Brazil/Uruguay)

- and Gariep (Namibia/South Africa) orogenic belts—evidence from a reconnaissance provenance study. *Precambrian Research*, **139**(3-4):195-221. <https://doi.org/10.1016/j.precamres.2005.06.005>
- Basei M.A.S., Peel E., Bettucci L.S., Preciozzi F., Nutman A.P. 2011. The basement of the Punta del Este Terrane (Uruguay): an African Mesoproterozoic fragment at the eastern border of the South American Rio de La Plata craton. *International Journal of Earth Sciences*, **100**(2):289-304. <https://doi.org/10.1007/s00531-010-0623-1>
- Beard J.S., Ragland P.C., Crawford M.L. 2005. Reactive bulk assimilation: A model for crust-mantle mixing in silicic magmas. *Geology*, **33**(8):681-684. <https://doi.org/10.1130/G21470.1>
- Bitencourt M.D.F., Nardi L.V.S. 2000. Tectonic setting and sources of magmatism related to the Southern Brazilian Shear Belt. *Revista Brasileira de Geociências*, **30**(1):186-189.
- Bossi J., Gaucher C. 2004. The Cuchilla Dionisio Terrane, Uruguay: an allochthonous block accreted in the Cambrian to SW-Gondwana. *Gondwana Research*, **7**(3):661-674. [https://doi.org/10.1016/S1342-937X\(05\)71054-6](https://doi.org/10.1016/S1342-937X(05)71054-6)
- Bossi J., Urquhart U. 1975. Magmatismo mesozoico de Uruguay y Rio Grande del Sur; sus recursos minerales asociados y potenciales. In: Congreso Iberoamericano de Geología Económica, 2., Buenos Aires. *Actas...* p. 119-142.
- Bühn B., Pimentel M.M., Matteini M., Dantas E.L. 2009. High spatial resolution analysis of Pb and U isotopes for geochronology by laser ablation multi-collector inductively coupled plasma mass spectrometry (LA-MC-ICP-MS). *Anais da Academia Brasileira de Ciências*, **81**(1):99-114. <https://doi.org/10.1590/S0001-37652009000100011>
- Charlier B.L.A., Wilson C.J.N., Lowenstern J.B., Blake S., van Calsteren P.W., Davidson J.P. 2005. Magma generation at a large, hyperactive silicic volcano (Taupo, New Zealand) revealed by U–Th and U–Pb systematics in zircons. *Journal of Petrology*, **46**(1):3-32. <https://doi.org/10.1093/ptrology/egh060>
- Clarke D.B. 2007. Assimilation of xenocrysts in granitic magmas: principles, processes, proxies, and problems. *The Canadian Mineralogist*, **45**(1):5-30. <https://doi.org/10.2113/gscanmin.45.1.5>
- Comin-Chiaromonti P. 2000. Peraluminous lavas from Jaguarão (Rio Grande do Sul, Brazil). DICAMP: Quaderni di Mineralogia, Petrografia e Geochimica Applicata, Trieste University 17.
- Comin-Chiaromonti P., Gomes C.B. 2005. *Mesozoic to Cenozoic alkaline magmatism in the Brazilian Platform*. São Paulo: EdUSP.
- Comin-Chiaromonti P., Riccomini C., Slejko F., De Min A., Ruberti E., Gomes C.B., 2010. Cordierite-bearing lavas from Jaguarão, southern Brazil: petrological evidence for crustal melts during early rifting of Gondwana. *Gondwana Research*, **18**(2-3):514-527. <https://doi.org/10.1016/j.gr.2009.12.007>
- Cooper K.M., Kent A.J. 2014. Rapid remobilization of magmatic crystals kept in cold storage. *Nature*, **506**(7489):480-483. <https://doi.org/10.1038/nature12991>
- Cruz R.F. 2019. *Projeto sudeste do Rio Grande do Sul: escalas 1: 250.000 e 1: 100.000; estado do Rio Grande do Sul*. Porto Alegre: CPRM, 173 p.
- Davidson J.P., Morgan D.J., Charlier B.L.A., Harlou R., Hora J.M. 2007. Microsampling and isotopic analysis of igneous rocks: implications for the study of magmatic systems. *Annual Review of Earth and Planetary Science*, **35**:273-311. <https://doi.org/10.1146/annurev.earth.35.031306.140211>
- Davis W.J., Canil D., MacKenzie J.M., Carbone G.B. 2003. Petrology and U–Pb geochronology of lower crustal xenoliths and the development of a craton, Slave Province, Canada. *Lithos*, **71**(2-4):541-573. [https://doi.org/10.1016/S0024-4937\(03\)00130-0](https://doi.org/10.1016/S0024-4937(03)00130-0)
- Fragoso-César A.R.S. 1986. O batólito Pelotas (Proterozoico superior/Eopaleozoico) no Escudo do Rio Grande do Sul. In: Congresso Brasileiro de Geologia, 34. *Anais...* SBG, p. 1322-1343.
- Frantz J.C., Botelho N.F. 2000. Neoproterozoic granitic magmatism and evolution of the eastern Dom Feliciano Belt in southernmost Brazil: a tectonic model. *Gondwana Research*, **3**(1):7-19. [https://doi.org/10.1016/S1342-937X\(05\)70053-8](https://doi.org/10.1016/S1342-937X(05)70053-8)
- Frantz J.C., McNaughton N.J., Marques J., Hartmann L., Botelho N.F., Caravaca G. 2003. Shrimp U–Pb zircon ages of granitoids from southernmost Brazil: constraints on the temporal evolution on the Dorsal do Canguçu transcurrent shear zone and the eastern Dom Feliciano Belt. In: South American Symposium of Isotope Geology, 4. *Anais...*
- Gehrels G. 2014. Detrital zircon U–Pb geochronology applied to tectonics. *Annual Review of Earth and Planetary Sciences*, **42**:127-149. <https://doi.org/10.1146/annurev-earth-050212-124012>
- Gregory T.R., Fátima Bitencourt M., Nardi L.V.S., Florisbal L.M., Chemale Jr. F. 2015. Geochronological data from TTG-type rock associations of the Arroio dos Ratos Complex and implications for crustal evolution of southernmost Brazil in Paleoproterozoic times. *Journal of South American Earth Sciences*, **57**:49-60. <https://doi.org/10.1016/j.jsames.2014.11.009>
- Harley S.L., Kelly N.M. 2007. Zircon tiny but timely. *Elements*, **3**(1):13-18. <https://doi.org/10.2113/gselements.3.1.13>
- Höfig D.F., Marques J.C., Basei M.A.S., Giusti R.O., Kohlrausch C., Frantz J.C. 2018. Detrital zircon geochronology (U–Pb LA-ICP-MS) of syn-orogenic basins in SW Gondwana: New insights into the Cryogenian-Ediacaran of Porongos Complex, Dom Feliciano Belt, southern Brazil. *Precambrian Research*, **306**:189-208. <https://doi.org/10.1016/j.precamres.2017.12.031>
- Iglesias C.M.D.F., Camozzato E., Klein C., Laux J.H. 2018. *Geologia e recursos minerais da folha Curral de Pedras, SI. 22V-AI*.
- Jackson S.E., Pearson N.J., Griffin W.L., Belousova E.A. 2004. The application of laser ablation-inductively coupled plasma-mass spectrometry to in situ U–Pb zircon geochronology. *Chemical Geology*, **211**(1-2):47-69. <https://doi.org/10.1016/j.chemgeo.2004.06.017>
- Jerram D.A., Davidson J.P. 2007. Frontiers in textural and microgeochemical analysis. *Elements*, **3**(4):235-238. <https://doi.org/10.2113/gselements.3.4.235>
- Jerram D.A., Martin V.M. 2008. Understanding crystal populations and their significance through the magma plumbing system. Geological Society, London, Special Publications, **304**(1):133-148. <https://doi.org/10.1144/SP304.7>
- Kuritani T., Kitagawa H., Nakamura E. 2005. Assimilation and fractional crystallization controlled by transport process of crustal melt: implications from an alkali Basalt-Dacite Suite from Rishiri Volcano, Japan. *Journal of Petrology*, **46**(7):1421-1442. <https://doi.org/10.1093/ptrology/egi021>
- Ludwig K.R. 2003. *Isoplot 3.00: A geochronological toolkit for Microsoft Excel*. Berkeley Geochronology Center Special Publication, 4, 70 p.
- Maier W.D., Arndt N.T., Curl E.A. 2000. Progressive crustal contamination of the Bushveld Complex: evidence from Nd isotopic analyses of the cumulate rocks. *Contributions to Mineralogy and Petrology*, **140**(3):316-327. <https://doi.org/10.1007/s004100000186>
- McBirney A.R., Yoder H.S. 2015. Effects of assimilation. In: Bowen N.L. (ed.). *Evolution of the Igneous Rocks* (p. 307-338). Princeton: Princeton University Press.
- Misuzaki A. 1998. *Rochas ígneas básicas do Neocomiano da Bacia de Campos: características e comportamento como reservatório de hidrocarbonetos*.
- Oriolo S., Oyhantçabal P., Basei M.A., Wemmer K., Siegesmund S. 2016. The Nico Pérez Terrane (Uruguay): From Archean crustal growth and connections with the Congo Craton to late Neoproterozoic accretion to the Rio de la Plata Craton. *Precambrian Research*, **280**:147-160. <https://doi.org/10.1016/j.precamres.2016.04.014>
- Oriolo S., Oyhantçabal P., Konopásek J., Basei M.A., Frei R., Sláma J., Wemmer K., Siegesmund S. 2019. Late Paleoproterozoic and Mesoproterozoic magmatism of the Nico Pérez Terrane (Uruguay): tightening up correlations in southwestern Gondwana. *Precambrian Research*, **327**:296-313. <https://doi.org/10.1016/j.precamres.2019.04.012>
- Oyhantçabal P., Siegesmund S., Wemmer K. 2011. The Rio de la Plata Craton: a review of units, boundaries, ages and isotopic signature. *International Journal of Earth Sciences*, **100**(2-3):201-220. <https://doi.org/10.1007/s00531-010-0580-8>
- Philipp R.P., Machado R. 2002. Ocorrência e significado dos septos do embasamento encontrados nas suítes graníticas do Batólito Pelotas, RS, Brasil. *Pesquisas em Geociências*, **29**(1):43-60. <https://doi.org/10.22456/1807-9806.19597>
- Ramos R.C. 2014. *Evolução petrogenética e geotectônica do Ofolito Arroio Grande, SE do Cinturão Dom Feliciano (Brasil)*. Tese (Doutorado). Porto Alegre: Universidade Federal do Rio Grande do Sul.

- Reiners P.W., Nelson B.K., Ghiorso M.S. 1995. Assimilation of felsic crust by basaltic magma: thermal limits and extents of crustal contamination of mantle-derived magmas. *Geology*, **23**(6), 563-566. [https://doi.org/10.1130/0091-7613\(1995\)023%3C0563:AOFcBB%3E2.3.CO;2](https://doi.org/10.1130/0091-7613(1995)023%3C0563:AOFcBB%3E2.3.CO;2)
- Rosa M.L.C.D.C., Tomazelli L.J., Costa A.F.U., Barboza E.G. 2009. Integração de métodos potenciais (gravimetria e magnetometria) na caracterização do embasamento da região sudoeste da Bacia de Pelotas, sul do Brasil. *Revista Brasileira de Geofísica*, **27**(4):641-657. <https://doi.org/10.1590/S0102-261X2009000400008>
- Rudnick R.L., Williams I.S. (1987). Dating the lower crust by ion microprobe. *Earth and Planetary Science Letters*, **85**(1-3):145-161. [https://doi.org/10.1016/0012-821X\(87\)90028-8](https://doi.org/10.1016/0012-821X(87)90028-8)
- Saalmann K., Gerdes A., Lahaye Y., Hartmann L.A., Remus M.V.D., Läufer A. 2011. Multiple accretion at the eastern margin of the Rio de la Plata craton: the prolonged Brasiliano orogeny in southernmost Brazil. *International Journal of Earth Sciences*, **100**(2-3):355-378. <https://doi.org/10.1007/s00531-010-0564-8>
- Schmitz M.D., Bowring S.A. 2001. The significance of U-Pb zircon dates in lower crustal xenoliths from the southwestern margin of the Kaapvaal craton, southern Africa. *Chemical Geology*, **172**(1-2):59-76. [https://doi.org/10.1016/S0009-2541\(00\)00236-9](https://doi.org/10.1016/S0009-2541(00)00236-9)
- Silva L.C., Hartmann L.A., Mcnaughton N.J., Fletcher I.R. 1999. SHRIMP U-Pb zircon dating of Neoproterozoic granitic magmatism and collision in the Pelotas Batholith, southernmost Brazil. *International Geology Review*, **41**(6):531-551. <https://doi.org/10.1080/00206819909465156>
- Solano J.M.S., Jackson M.D., Sparks R.S.J., Blundy J.D., Annen C. 2012. Melt segregation in deep crustal hot zones: a mechanism for chemical differentiation, crustal assimilation and the formation of evolved magmas. *Journal of Petrology*, **53**(10):1999-2026. <https://doi.org/10.1093/ptrology/egs041>
- Sparks R.S.J. 1986. The role of crustal contamination in magma evolution through geological time. *Earth and Planetary Science Letters*, **78**(2-3):211-223. [https://doi.org/10.1016/0012-821X\(86\)90062-2](https://doi.org/10.1016/0012-821X(86)90062-2)
- Stacey J.T., Kramers J.D. 1975. Approximation of terrestrial lead isotope evolution by a two-stage model. *Earth and Planetary Science Letters*, **26**(2):207-221. [https://doi.org/10.1016/0012-821X\(75\)90088-6](https://doi.org/10.1016/0012-821X(75)90088-6)
- Streck M.J. (2008). Mineral textures and zoning as evidence for open system processes. *Reviews in Mineralogy and Geochemistry*, **69**(1):595-622. <https://doi.org/10.2138/rmg.2008.69.15>
- Tambara G.B., Koester E., Ramos R.C., Porcher C.C., Vieira D.T., Fernandes L.A.D.Á., Cristine L.E.N.Z. (2019). Geoquímica e geocronologia dos Gnaisses Piratini: magmatismo cálcio-alcálico médio a alto-K de 784 Ma (U-Pb SHRIMP) no SE do Cinturão Dom Feliciano (RS, Brasil). *Pesquisas em Geociências*, **46**(2):e0769. <https://doi.org/10.22456/1807-9806.95466>
- Tang H., Zheng J., Griffin W.L., O'Reilly S.Y., Yu C., Pearson N.J., Ping X., Xia B., Yang H. 2014. Complex evolution of the lower crust beneath the southeastern North China Craton: the Junan xenoliths and xenocrysts. *Lithos*, **206-207**:113-126. <https://doi.org/10.1016/j.lithos.2014.07.018>
- Umpierre M., Halpern M. 1971. Edades Sr-Rb del Sur de la República Oriental del Uruguay. *Revista Asociación Geológica Argentina*, **26**:133-155.
- Vermeesch P. 2018. IsoplotR: A free and open toolbox for geochronology. *Geoscience Frontiers*, **9**(5):1479-1493. <https://doi.org/10.1016/j.gsf.2018.04.001>
- Vieira D.T., Koester E., Bertotti A.L. 2016. Petrologia do Granito Chasqueiro, região de Arroio Grande, sudeste do Escudo Sul-Rio-Grandense. *Brazilian Journal of Geology*, **46**(1):79-108. <https://doi.org/10.1590/2317-4889201620150041>
- Vieira D.T., Koester E., Ramos R.C., Porcher C.C. 2019. Sr-Nd-Hf isotopic constraints and U-Pb geochronology of the Arroio Pedrado Gneisses, Dom Feliciano Belt, Brazil: A 680 Ma shoshonitic event in the final stages of The Piratini Arc evolution. *Journal of South American Earth Sciences*, **95**:102294. <https://doi.org/10.1016/j.jsames.2019.102294>
- Vieira Jr. N. 1985. *Petrologia e eoquímica do vulcanismo Mesozóico de Jaguarão*—RS. MS Dissertation, Universidade Federal do Rio Grande do Sul, Porto Alegre.
- Vieira Jr. N., Roisenberg A. 1987. Formação Jaguarão: uma nova unidade vulcânica mesozóica no Rio Grande do Sul. *Pesquisas em Geociências*, **19**(19):81-94. <https://doi.org/10.22456/1807-9806.21683>
- Watson E.B. 1996. Dissolution, growth and survival of zircons during crustal fusion: kinetic principals, geological models and implications for isotopic inheritance. *Earth and Environmental Science Transactions of the Royal Society of Edinburgh*, **87**(1-2):43-56. <https://doi.org/10.1017/S0263593300006465>
- Wildner W., Ramgrab G.E., Lopes R.D.C., Iglesias C.M.D.F. 2008. *Geologia e recursos minerais do estado do Rio Grande do Sul*. CPRM. 1 DVD. Escala 1:750.000. Programa Geologia do Brasil; Mapas Geológicos Estaduais.
- Yao Z., Mungall J.E., Jenkins M.C. 2021. The Rustenburg Layered Suite formed as a stack of mush with transient magma chambers. *Nature Communications*, **12**(1):505. <https://doi.org/10.1038/s41467-020-20778-w>
- Youden W.J. 1951. *Statistical methods for chemists*. New York: Wiley.